

# An ANFIS Control Approach of a Bi-Directional Buck-Boost used for a Battery Charger

Tsilavy Randjaka<sup>1</sup>, Solofanja Jeannie Rajonirina<sup>2</sup>, F. Philibert Andriniriniaimalaza<sup>3</sup> and Jean Nirinarison Razafinjaka<sup>4</sup>

<sup>1</sup>EDT ENRE, University of Antsiranana, Antsiranana, MADAGASCAR

<sup>2</sup>EDT ENRE, University of Antsiranana, Antsiranana, MADAGASCAR

<sup>3</sup>Higher Institute of Sciences and Technologies, University of Mahajanga, Mahajanga, MADAGASCAR

<sup>4</sup>Higher Polytechnic School, University of Antsiranana, Antsiranana, MADAGASCAR

<sup>1</sup>Corresponding Author: tsilavy@gmail.com

## ABSTRACT

In this work, a neuro-fuzzy regulator based on ANFIS is designed for the current control of a Bidirectional Buck-Boost chopper battery charger. First, a PI regulator is used in the control loop. Data from the PI regulator is extracted and then used to train ANFIS. The performances of the two PI and neuro-fuzzy commands were evaluated under the MATLAB/SIMULINK environment. According to the simulation results, it was found that the neuro-fuzzy regulator ANFIS is more effective in improving the current response by reducing the response time. In conclusion, the neuro-fuzzy control gives a better performance compared to the PI control.

**Keywords--** Buck-Boost, Bidirectional, PI, Neuro-fuzzy, ANFIS

[3], [4] and [5].

In this work, we propose to design for a bidirectional Buck-Boost chopper, a neuro-fuzzy control based on the hybrid neuro-fuzzy model ANFIS in order to compare the performance of a neuro-fuzzy controller with a PI controller classic.

The following plan is considered: Section 2 consists of the modeling of the Buck-Boost chopper. Section 3 presents the design procedures for PI and neuro-fuzzy controls. The simulation results of the two control strategies are compared in section 4. Finally, conclusions are given in section 5. In the recent years, rapid transition has been observed in research in computer vision and machine learning.

## I. INTRODUCTION

One of the applications of a bi-directional chopper is in PV systems with storage battery. The chopper constitutes the interface between the DC bus and the battery, and thus allows the control of the charge and the discharge of the battery by controlling the current in its inductance. For current control of these choppers, a PI controller is traditionally used as presented in [1], [2],

## II. BIDIRECTIONAL BUCK-BOOST MODELING

### 2.1 System Overview

Figure 1 presents the structure of the bidirectional Buck-Boost chopper associated with a battery. The battery model is likened to a DC voltage source fitted with a variable resistor representing the internal resistance of the battery [6].

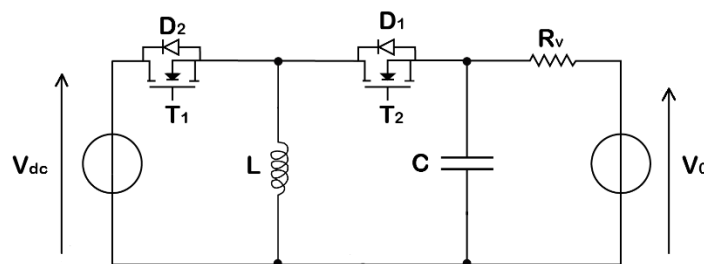


**Figure 1:** Bidirectional Buck-Boost Converter associated with a battery.

In this assembly,  $T_1$  and  $T_2$  are actuated in a synchronous and complementary mode, which is to say, when  $T_1$  is closed,  $T_2$  is open and vice versa.

It therefore appears two operating sequences of the chopper according to the states of  $T_1$  and  $T_2$ :

- Sequence 1:  $T_1$  closed  $\Rightarrow T_2$  open

$$L \frac{di_L}{dt} = V_{dc} \tag{1}$$

$$0 = C \frac{dV_c}{dt} + \frac{(V_c + V_0)}{R_v} \tag{2}$$

- Sequence 2:  $T_1$  open  $\Rightarrow T_2$  closed

$$L \frac{di_L}{dt} = -V_c \tag{3}$$

$$i_L = C \frac{dV_c}{dt} + \frac{(V_c + V_0)}{R_v} \tag{4}$$

Let be  $c(t)$  the control state of  $T_1$  during its commutation, and  $1-c(t)$  that of  $T_2$ . When  $T_1$  is closed

and  $T_2$  is open,  $c(t)=1$ . For  $T_1$  open and  $T_2$  closed,  $c(t)=0$ .

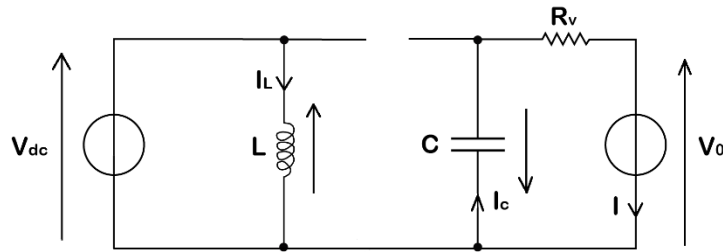


Figure 2: Operation sequence 1

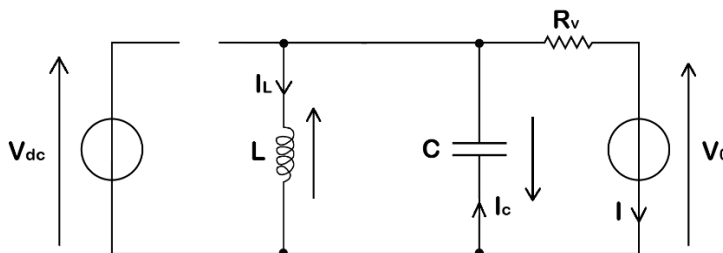


Figure 3: Operation sequence 2

Thus, by analyzing the two operating sequences of the chopper, we obtain the model under ideal conditions defined by the following two differential equations:

$$L \frac{di_L}{dt} = c(t)V_{dc} - (1-c(t))V_c \quad (5)$$

$$(1-c(t))i_L = C \frac{dV_c}{dt} + \frac{(V_c + V_o)}{R_v} \quad (6)$$

Since components are never perfect in practice, an internal resistance  $R_L$  to inductance  $L$  can be added.

Then, equation (5) then becomes:

$$L \frac{di_L}{dt} + R_L i_L = c(t)V_{dc} - (1-c(t))V_c \quad (7)$$

### 2.2 Structure of the Current Control loop

The chopper current control loop contains four blocks (Figure 4).

- Regulator

Its role is to act on the control variable  $u$  to make the measured current value  $I_L$  as close as possible to the setpoint value  $I_{ref}$  and thus minimize the current error  $e$ .

- Limitation

This block will limit the quantity  $u$  produced by the regulator between 0 and 1, knowing that the cyclic ratio  $\alpha$  of the chopper must be included in this interval.

- Pulse Width Modulator (PWM)

It receives the duty cycle at its input  $\alpha$  and outputs slots 0-1 and

$$e = I_{ref} - I_L \quad (8)$$

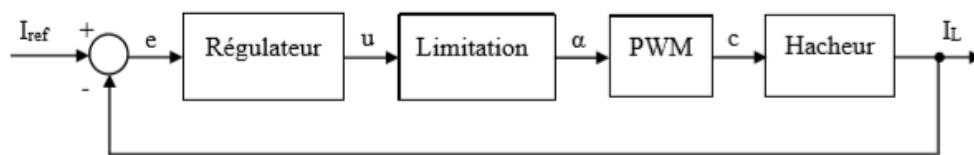


Figure 4: Current control loop of Buck-Boost converter

## III. ORDERING STRATEGIES, DESIGN AND SYNTHESIS

### 3.1. PI Control

- Structure adopted

The PI regulator used here is of the product form

which is written:

$$G_R(p) = \frac{1 + pT_n}{pT_i} \quad (9)$$

With  $T_n$ , the integral correlation assay and  $T_i$ , the

integral time constant.

- Design and synthesis of the regulator

According to equation (7) of the modeling of the Buck-Boost chopper, we have a first-order system whose transfer function that we denote  $G(p)$  with its expression:

$$G(p) = \frac{1}{1 + p \frac{L}{R_L}} \quad (10)$$

For a static gain and a time constant of the system named respectively  $K$  and  $T$ , we have:

$$G(p) = \frac{K}{1 + pT} \tag{11}$$

Where:

$$\begin{cases} K = \frac{1}{R_L} \\ T = \frac{L}{R_L} \end{cases} \tag{12}$$

The open loop transfer function (FBTO) is then:

$$G_0(p) = G_r(p).G(p) = \frac{1 + pT_n}{pT_i} \cdot \frac{K}{1 + pT} \tag{13}$$

By the General Method [7], we have:

$$\begin{cases} T_n = aT \\ T_i = bKT \\ a > 0; b > 0 \end{cases} \tag{14}$$

For  $a=1$ , the FTBO becomes:

$$G_0(p) = G_r(p).G(p) = \frac{1 + pT}{pbK} \cdot \frac{K}{1 + pT} = \frac{1}{pbT} \tag{15}$$

The closed loop transfer function (FTBF) will be:

$$H(p) = \frac{1}{1 + pbT} \tag{16}$$

According to this equation, the response is all the more rapid as  $b$  decreases ( $0 < b < 1$ ).

### 3.2. Neuro-fuzzy Control based on ANFIS

- Preparation of the order

Figure 5 below describes the elaboration of the neuro-fuzzy control based on the learning of the current PI regulator in the control loop [8], [9].

In this scheme, the hybrid neuro-fuzzy model ANFIS is used to make an offline identification of the PI regulator. Once this identification is accomplished, the neuro-fuzzy network replaces the regulator in the control loop and will function as a current neuro-fuzzy regulator.

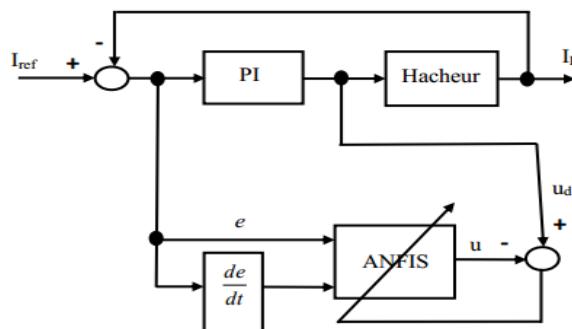


Figure 5: ANFIS structure system

- ANFIS model used

Figure 9 presents the ANFIS architecture that we used. The model contains 9 rules. The two system

inputs are the current error  $e$  and the variation of the current error  $e$ , and at output the command  $u$ .

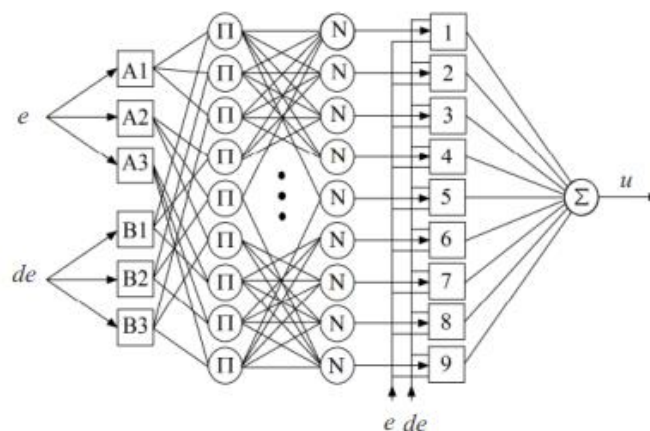


Figure 6: ANFIS off-line training

- Layer1: This is the fuzzification layer. The membership functions are of the Gaussian form.

$$\mu_{A_i}(e) = \exp\left(-\frac{(e-a_i)^2}{2b_i^2}\right); i = 1, 2, 3 \tag{18}$$

$$\mu_{B_i}(de) = \exp\left(-\frac{(de-c_i)^2}{2d_i^2}\right); i = 1, 2, 3 \tag{19}$$

Where  $(a_i, b_i)$  and  $(c_i, d_i)$  are the parameters of the rule premises.

- Layer 2: The neurons in this layer model the “AND” operator and calculate the truth value of each rule.

$$w_j = \mu_{A_i}(e) \times \mu_{B_i}(de); i = 1, 2, 3; j = 1, 2, \dots, 9 \tag{20}$$

- Layer3: This is the normalization layer of the truth value of each rule.

$$\bar{w}_i = \frac{w_i}{\sum_i w_i}; i = 1, 2, \dots, 9 \tag{21}$$

- Layer 4: Each neuron in this layer has the function of:

$$\bar{w}_i f_i = \bar{w}_i (p_i e + q_i de + r_i); i = 1, 2, \dots, 9 \tag{22}$$

Or  $(p_i, q_i, r_i)$  are the parameters of the consequences of the rules.

- Layer5: The neuron in this layer delivers the network output given by:

$$u = \sum_i \bar{w}_i f_i; i = 1, 2, \dots, 9 \tag{23}$$

The parameters of ANFIS which are the parameters of the premises and the parameters of the consequences are optimized by using the hybrid learning method formed by the combination of the gradient descent algorithm and the least squares estimation algorithm [10].

### IV. SIMULATIONS AND RESULTS

#### 4.1. Simulations and Parameters Used

- Simulations

Under Matlab/Simulink, the model below was adopted during the various simulations.

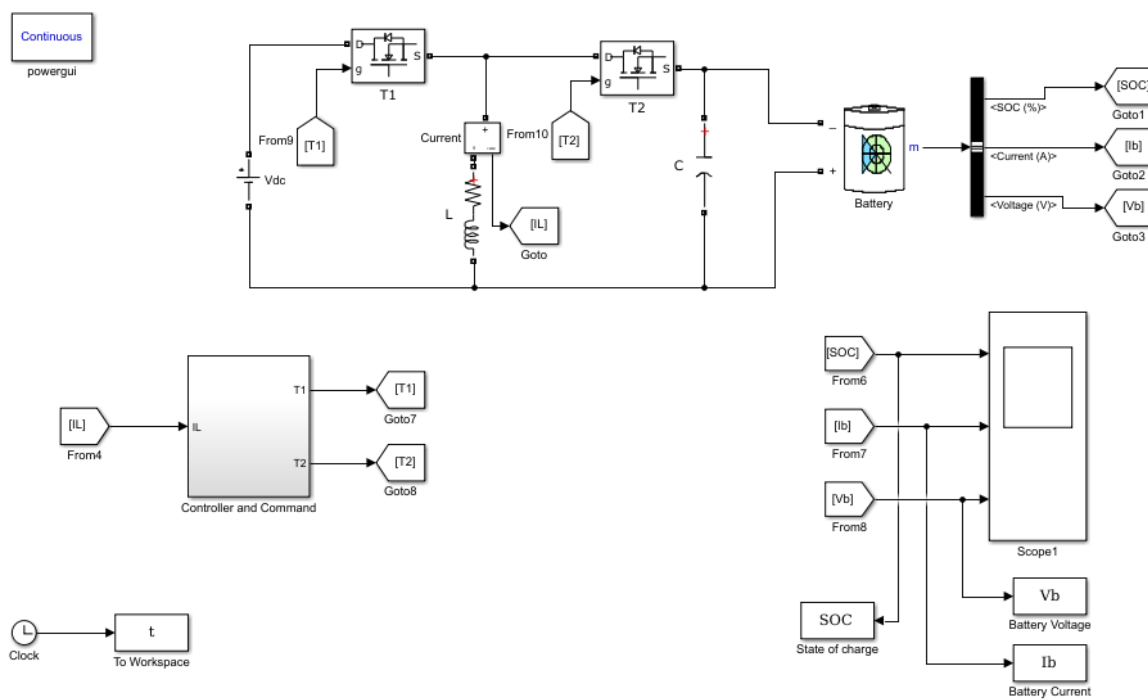
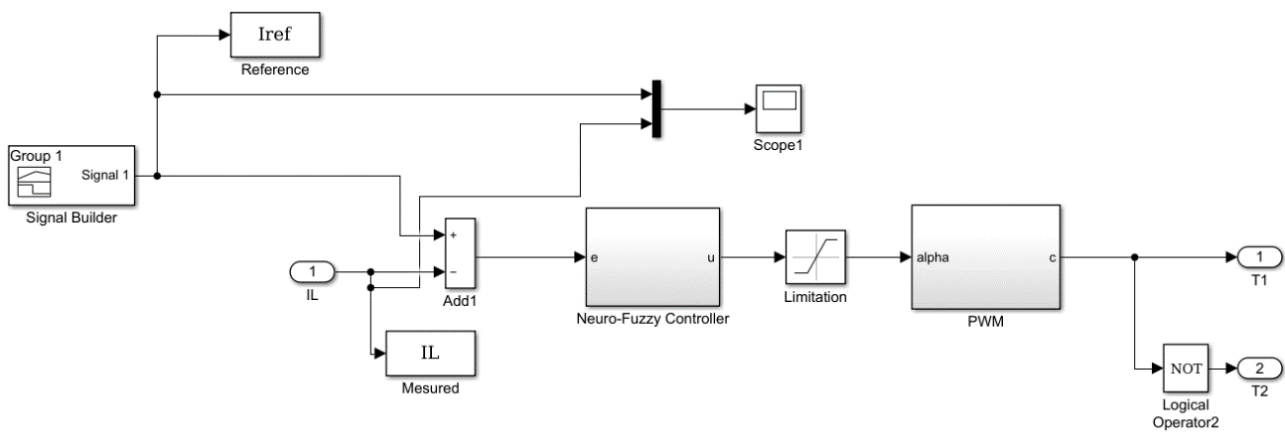
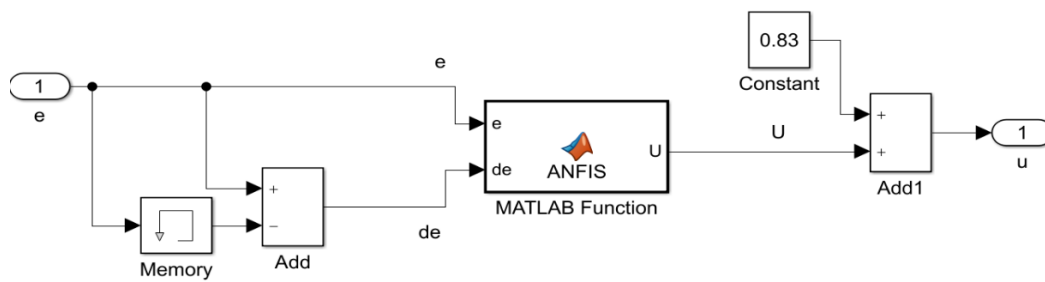


Figure 7: Bidirectional Buck-Boost converter with current loop control



**Figure 8:** Controller and Command with Neuro-Fuzzy controller



**Figure 9:** Internal structure of the Neuro-fuzzy Controller

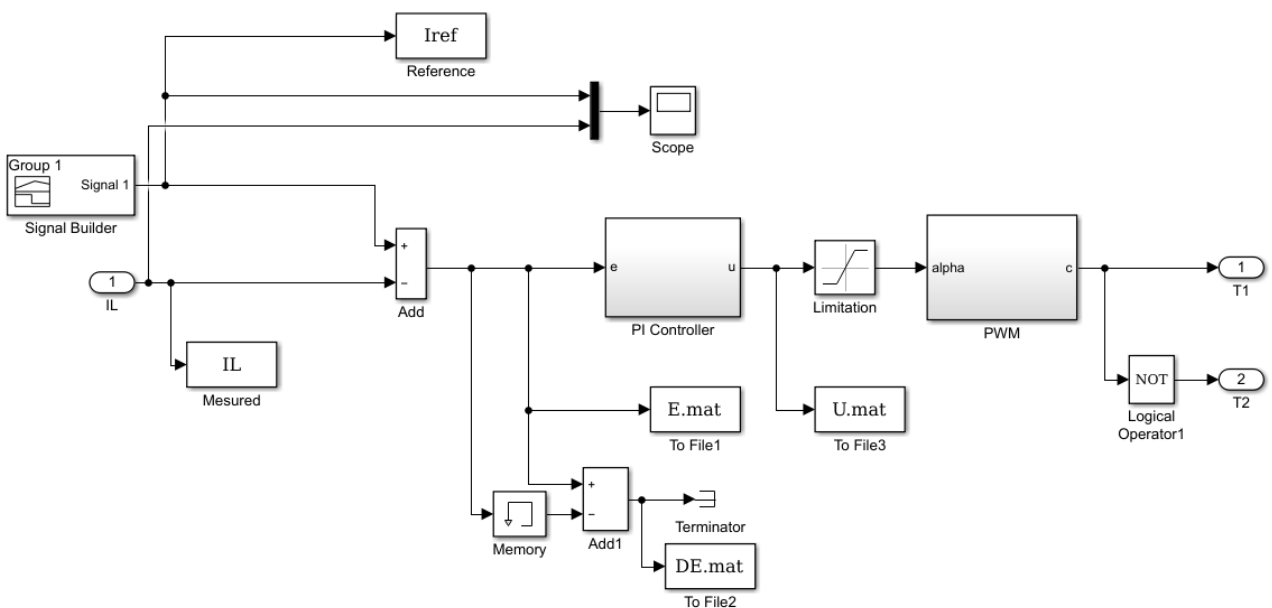


**Figure 10:** Data-gathering of ANFIS training

- ⇒ The 0.83 weighting coefficient mounted in parallel with the ANFIS regulator performs the integral action enabling the steady-state current error to be eliminated.
- ⇒ For a simulation duration of 1.5s, the current setpoint changes to -1A to  $t=0s$ , to then rise to 1A to  $t=0.37s$ , and then to 2A to  $t=0.74s$  to finally descend to 2A to  $t=1.11s$ .
- Parameters used

**Table 1:** Simulation parameters

Settings	Values
<b>Bidirectional Buck-Boost Chopper</b>	
Input voltage $V_{dc}$	24V
Switching frequency $f$	50KHz
Inductance $L$	1.3mH
Internal resistance $R_L$ to the inductor	0.1Ω
Capacitor $C$	1.3mH
<b>Battery</b>	
Li-ion type	
Nominal voltage	48V
Ability	10Ah
Initial SOC	50 %

**4.2. Case of the PI regulator**

$b=0.08, T_n=0.013s,$  and  $T_i=0.0104s.$

For the following PI controller parameters:  $a=1,$

We have the below simulation results:

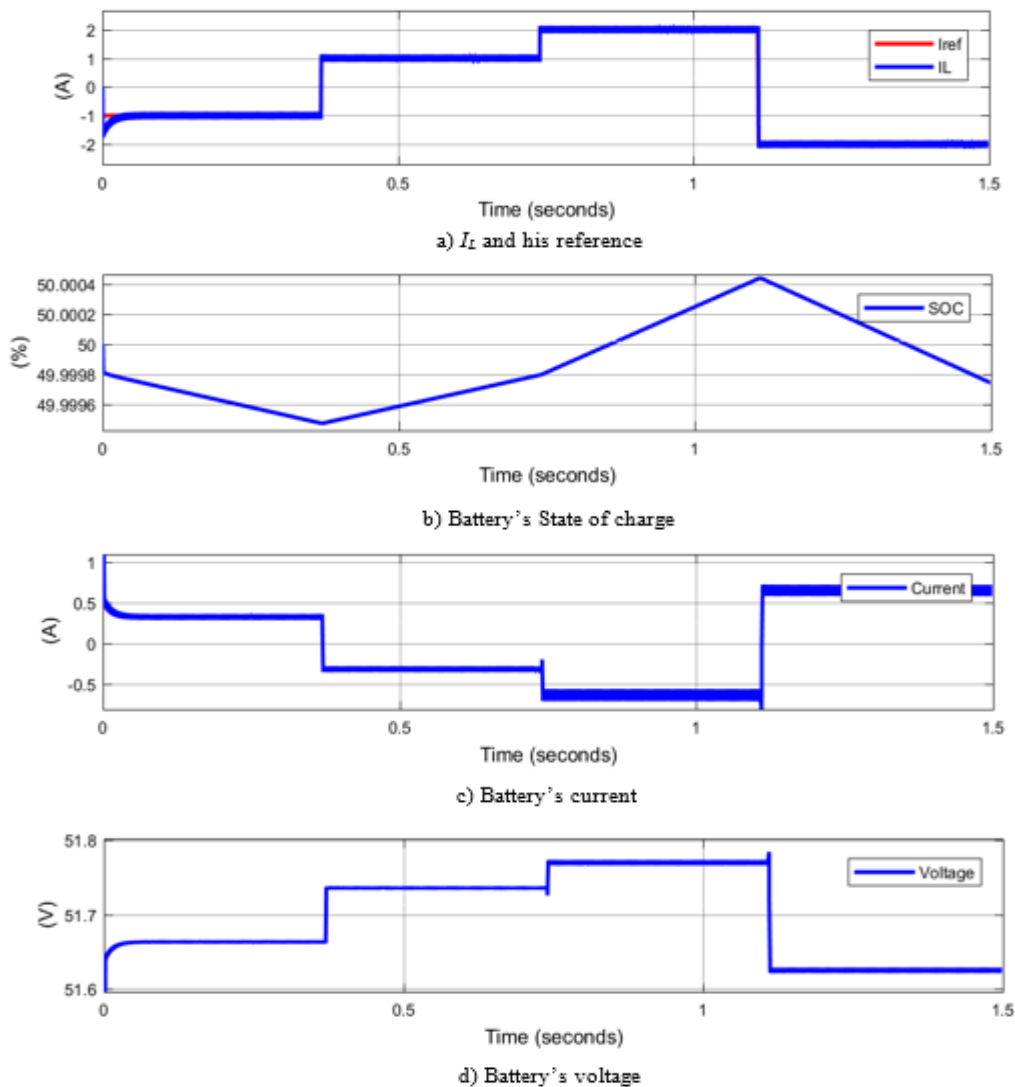


**Figure 11:** Simulation results with PI Controller

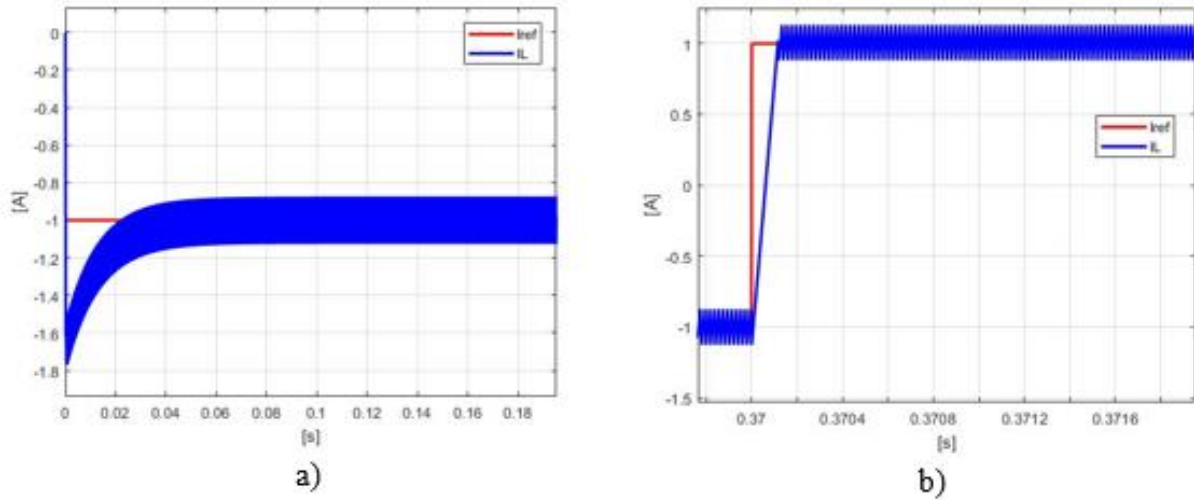


Figure 12: Zoom of the current with variations of reference, a) at -1[A] and b) at 1[A]

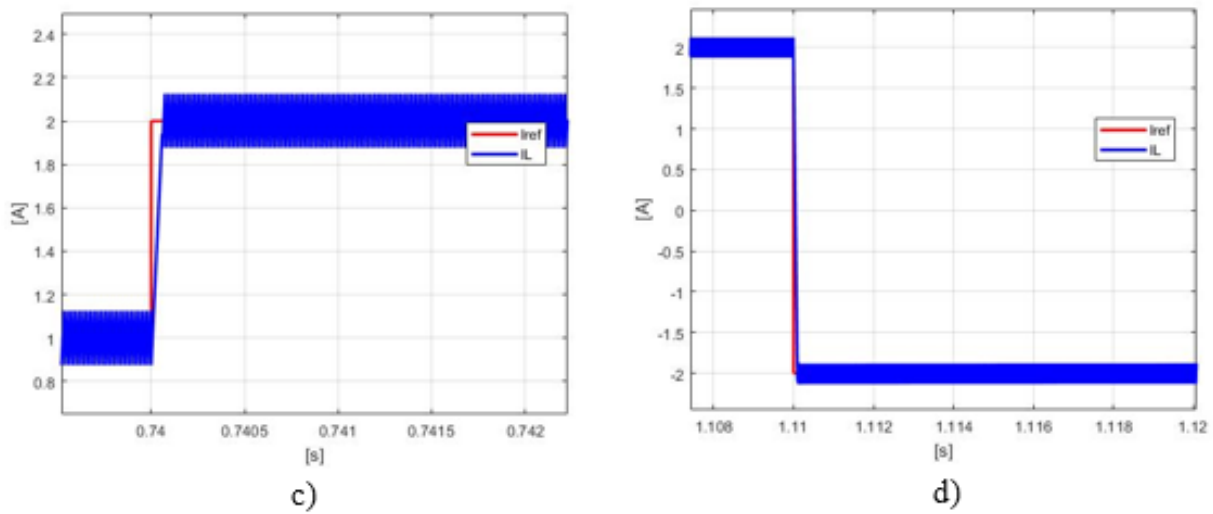


Figure 13: Zoom of the current with variations of reference, c) at 2[A] and d) at -2[A]

#### 4.3. Case of the Neuro-Fuzzy Regulator

With 100 input/output data pairs from the PI regulator, we have the learning curve in figure 15 below. At the 35th iteration, we have obtained the root of the

quadratic error  $RMSE = 6,2372 \times 10^{-4}$ . After optimization of the antecedent parameters and conclusions of the ANFIS rules, we have the next results

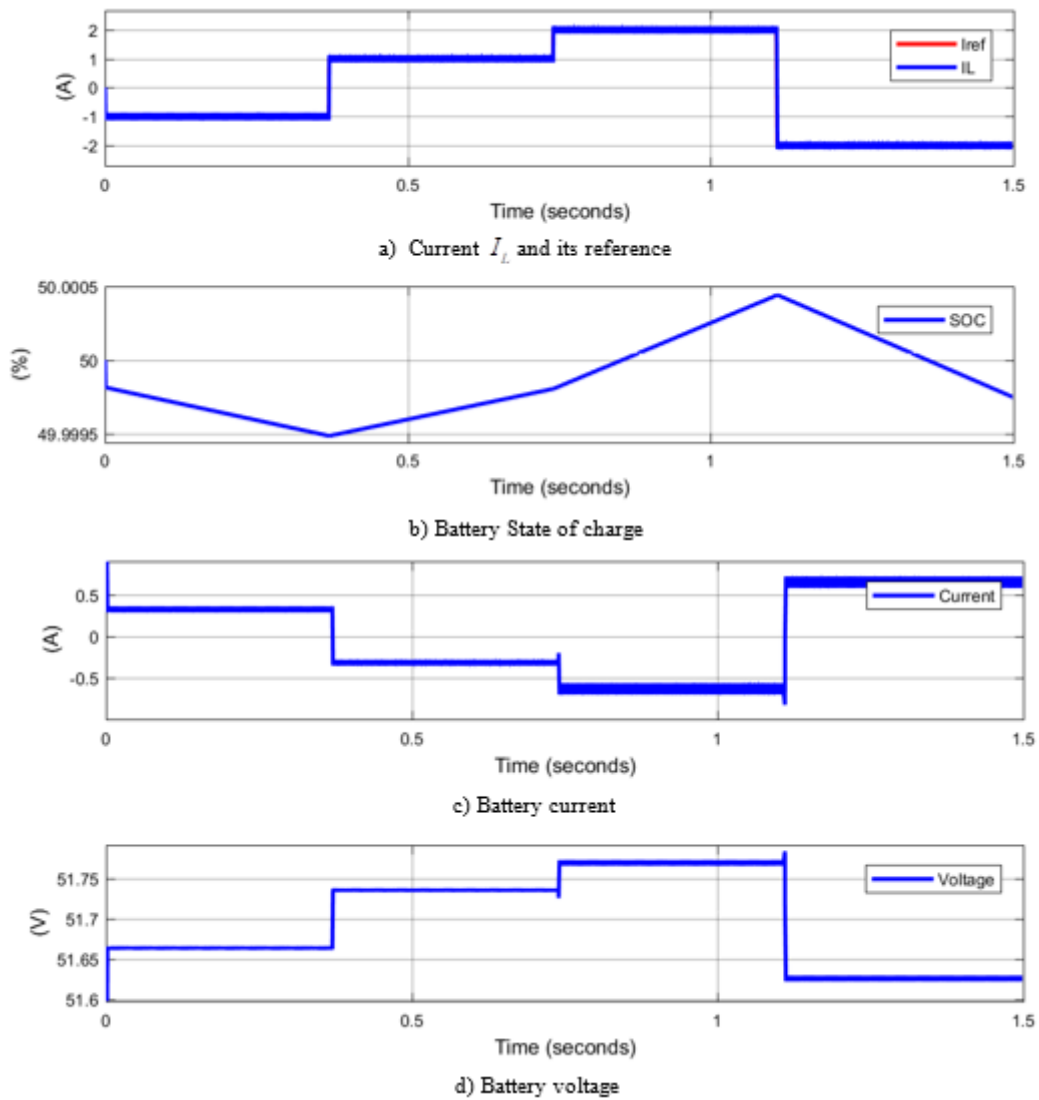


Figure 14: Simulation results with Neuro-Fuzzy controller

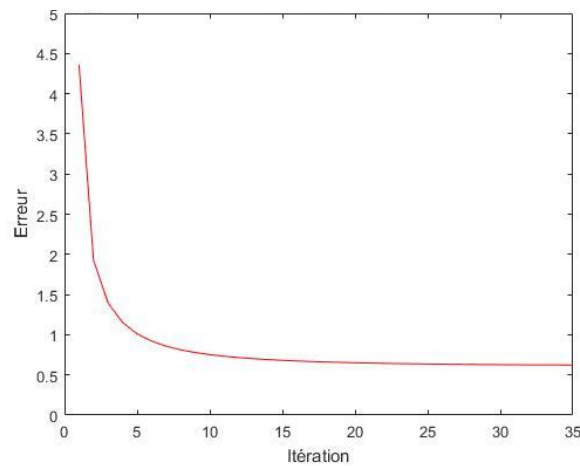
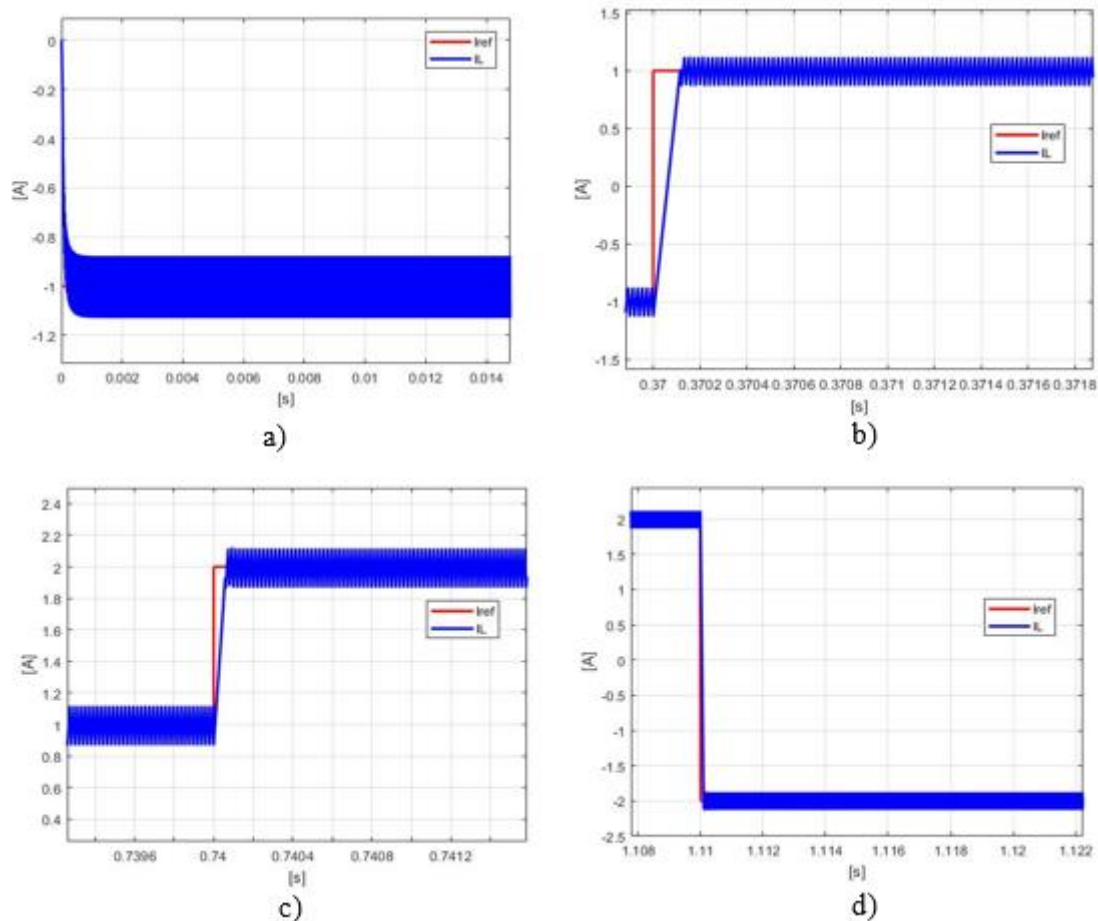


Figure 15: ANFIS training curve



**Figure 16:** Zoom of the current according to the references, a) at -1[A], b) at 1[A], c) at 2[A] and d) at -2[A]

According to figure 15.a, we can say that the current  $I_L$  of the chopper is well regulated and always follows the setpoint despite the variations of the latter. It can be seen that at the instants of variation of the setpoint, the current  $I_L$  is quickly brought back to it. It can also be seen, as in the case of the PI regulator, that the charging and discharging of the battery are well controlled. In Figure 16, the current response has response times of

$t=0.01s$ ,  $t=0.37015s$ ,  $t=0.7401s$ ,  $t=1.1101s$  for setpoints which are respectively -1A, 1A, 2A and -2A.

### V. DISCUSSIONS

Table 2 summarizes the performance results in terms of speed of both PI and neuro-fuzzy controls.

**Table 2:** Comparative table of PI and neuro-fuzzy commands

Reference/ Time	Response time (s)	
	IP	Neuro-Fuzzy
-1A at $t=0s$	0.08	0.001
1A, to $t=0.37s$	0.37015	0.37015
2A to $t=0.74s$	0.7401	0.7401
-2A at $t=1.11s$	1.111	1.1101

It can be seen from this table that for the two commands, there are the same response times for each setpoint change to  $t=0.37s$  and  $t=0.74s$ .

For setpoint changes at  $t=0s$  and  $t=1.11s$ : the

Buck-Boost current is established at the value -1A after  $t=0.001s$  and at the value -2A after  $t=1.1101s$  with the neuro-fuzzy regulator, while that of the PI regulator only reaches the value -1A after  $t=0.08s$  and the value -2A after

$t=1.111s$ .

Then, compared to the PI control, the neuro-fuzzy control shows a decrease of  $0.9ms$  and of  $79ms$  in terms of response time for the set point changes which are respectively at  $t=0s$  and  $t=1.111s$ . The current response is faster with the neuro-fuzzy regulator because there is a reduction in the response time. Then, the use of the neuro-fuzzy control improves the response of the system compared to the PI control at the level of the response time of the system.

## VI. CONCLUSION

In this work, a neuro-fuzzy control based on ANFIS of a bidirectional Buck-Boost chopper battery charger was designed and compared to a PI control. The necessary training data was collected from the PI control regulator. The simulation results showed that compared to the PI control, the neuro-fuzzy control gives a better performance on the current control of a bidirectional Buck-Boost chopper with minimal response times for all the set point variations.

## REFERENCES

- [1] El Hadji Mbaye Ndiaye , Alphousseyni Ndiaye , Mactar Faye & Samba Gueye. (2020). Intelligent control of a photovoltaic generator for charging and discharging battery using adaptive neuro-fuzzy inference system. *International Journal of Photoenergy*, 2020, ID 8649868.
- [2] Amara Yasmine, Bradai Rafik, Boukenoui Rachid & Mellit Adel. (2020). *Management of hybrid pv/battery stand-alone system under partial shading conditions*. 978-1-7281-5835-8/20/S31.00 IEEE
- [3] S. Boukebbous & D. Kerdoun. (2017). Power management of grid connected photovoltaic installation assisted by batteries and water pumping energy storage in desert location. *International Journal of Renewable Energy Research*, 7(4).
- [4] N. Pooja & D. Krishna. (2021). Energy management system designed for residential grid connected micro grid. *Turkish Journal of Computer and Mathematics Education*, 12(3), 4627-4634.
- [5] M. Traore, A. Ndiaye, S. Mbodji and al. (2018). *Supervision of a PV system with storage connected to the power line and design of a battery protection system*. DOI: 10.1007/s11276-018-1886-x.
- [6] Holiarimanga Mariette Randriamanjakony, Andrianantenaina Tsiory Patrick & Jean Nirinarison Razafinjaka. (2022). New PI controller design and applications. *International Journal of Engineering Research & Technology (IJERT)*, 11(04).
- [7] M. Bechouche Ali. (2013). Use of advanced techniques for the observation and control of an asynchronous machine: Application to a wind turbine. *Doctoral Thesis in Electrical Engineering, Mouloud Mammeri University of Tizi-Ouzou*.
- [8] Narendra Bawane, Anil G. Kothari & Dwarkadas P. Kothari. (2005). ANFIS based HVDC control and fault identification of HVDC converter. *HAIT Journal of Science and Engineering B*, 2(5-6), 673-689.
- [9] J.-SR Jangn C.-T. Sun & E. Mizutani. (1997). *Neuro-fuzzy and soft computing: a computational approach to learning and machine intelligence*. Upper Saddle River, NJ: Prentice Hall.